Macromolecules

Article

pubs.acs.org/Macromolecules

Local and Global Dynamics in Polypropylene Glycol/Silica Composites

R. Casalini and C. M. Roland*

Chemistry Division, Naval Research Laboratory, Washington, D.C. 20375-5342, United States

Supporting Information

ABSTRACT: The local segmental and global dynamics of a series of polypropylene glycol/silica nanocomposites were studied using rheometry and mechanical and dielectric spectroscopies. The particles cause substantial changes in the rheology, including higher viscosities that become non-Newtonian and the appearance of stress overshoots in the transient shear viscosity. However, no change was observed in the mean relaxation times for either the segmental or normal mode dynamics measured dielectrically. This absence of an effect of the particles is due to masking of the interfacial response by polymer chains remote from the particles. When the unattached polymer was extracted to isolate the interfacial material, very large reductions in both the local and global relaxation times were measured. This speeding up of the dynamics is due in part to the reduced density at the interface, presumably a consequence of poorer packing of tethered chains. In addition, binding of the ether oxygens of the polypropylene glycol truncates the normal mode, which contributes an additional shift of the corresponding relaxation peak to higher frequencies.

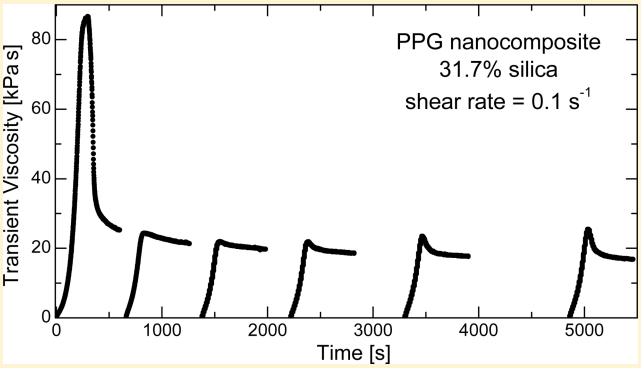

INTRODUCTION

Over the past decade there has been a plethora of activity directed to studying and exploiting polymer nanocomposites.[1−6] The mechanical and other properties of polymers can be greatly affected by the presence of small particles. In addition to redistributing strains locally (hydrodynamic interaction), particulate fillers can perturb the segmental dynamics, as manifested by changes in the temperature and intensity of the glass transition. Very generally, the expectation is that the polymer material comprising the interface with the particles will experience effects analogous to those observed in thin films, with the potential for additional effects due to specific interfacial interactions.[7−10]

Less work has been reported concerning the effect of nanoparticles on the global dynamics. The rheology of nanocomposites is of obvious import, given the enormous specific surface area of nanoparticles.[11,12] Frank et al.[13] observed substantial decreases in the lateral diffusion coefficient of polymer chains in thin films. On the other hand, Kremer et al.[14] observed no change in the normal-mode frequency for polyisoprene confined to thin films but did report the appearance of a new mode, ascribed to motion of subchains associated with chain segments confined at the interface. For nanocomposites of polymer blends, the viscosity in the vicinity of nanoparticles was reported to be lower than for the bulk material,[15] ascribed to alteration of the composition of the blend near the nanoparticle surface. It also appears that for high molecular weight polymers thin film confinement may cause a reduction in entanglements, with consequent decrease in viscosity and related rheological properties.[16−18] However, increased entanglements have also been observed in simulations,[19] and experimentally a reduced compliance was found for thin films of polystyrene.[20] The related problem of diffusion of polymer chains through nanopores has been studied theoretically and numerically by various groups.[21−25]

Generally, bulk measurements do not show large changes in the segmental dynamics or glass transition temperature, T_g, especially when the interfacial material represents only a small fraction of the total polymer.[26,27] The details of the particle−polymer interaction, as well as any density changes of the interfacial material, appear to be the dominant mechanisms for perturbation of the local dynamics. However, it is an experimental challenge to decouple the response of the interface from that of the bulk (unbound) material. The situation is similar to miscible blends, in which the components exert reciprocal influences, with the observed relaxation spectra reflecting intrinsic mobilities and intermolecular effects. Simulations can overcome the problem of the behavior of the interfacial material being swamped by that of the bulk, by enabling a focus on only those chains proximate to particles.[28−33] Simulations suggest that attraction to the particle surface expands the size of the interfacial chains,[34] presumably

Received: February 18, 2016
Revised: April 27, 2016
Published: May 3, 2016

DOI: 10.1021/acs.macromol.6b00354
Macromolecules 2016, 49, 3919−3924

affecting their motion. For the rheological properties, a reduction in entanglements can be the origin for enhanced mobility.[35]

One of the more common particulates for nanocomposites is silica. Various groups have reported at most only small effects on the local segmental dynamics of silica nanocomposites,[36−38,41] although there can be detectable changes on the lower frequency side of the segmental dispersion.[36] Cheng et al.[39] found increases in T_g and fragility in silica−glycerol mixtures, ascribed to densification of the interfacial region. Addition of silica nanoparticles was reported to reduce the intensity of the glass transition of poly(2-vinylpyridine) due to restricted segmental mobility of polymer segments at the interface;[40] on the other hand, for silica nanocomposites of poly(vinyl acetate) no change was observed in the magnitude of the property changes at T_g, beyond that due to the replacement of polymer by the filler.[41] Atomic force microscopy showed restricted mobility for styrene−butadiene copolymer at the interface with silica particles.[42] From quasielastic neutron scattering, Masui et al.[43] concluded that the primary effect of silica nanoparticles was a longer residence time between diffusive jumps.

In this work we investigate the effect of silica nanoparticles on polypropylene glycol (PPG). This particular polymer was chosen because it has a dipole moment parallel to the chain, which enables the global chain motions to be measured by dielectric spectroscopy. To resolve the dynamics at the interface, we extracted the unbound polymer. We find that after extraction the local segmental and the normal mode relaxation times are both reduced by the particulate reinforcement (i.e., faster dynamics); interestingly, the changes in the global motions are greater than the changes of the segmental dynamics. We also observe in steady shear experiments an overshoot peak in the transient viscosity of the nanocomposite at higher silica concentrations. This stress overshoot exhibits a delayed recovery after cessation and restarting the shear flow; the time scale for the full magnitude of the overshoot to be recovered is substantially longer than the relaxation time associated with the rheological properties. We ascribe this shear-induced structural change, which requires strains of ∼500%, to interactions between the silica particles.

EXPERIMENTAL SECTION

Polypropylene glycol (PPG) (weight-average molecular weight = 4000 Da) was obtained from Polysciences Inc. Because of its hydrophilic nature, care was taken to dry the material (by heating at 80 °C *in vacuo*) before measurements, and the latter were done either under vacuum or a dry nitrogen atmosphere. Silica (Si) nanoparticles (diameter ∼ 12.5 nm) were obtained from Nissan Chemicals. The particles are functionalized with hydroxyl groups (5−8 OH per nm^2) and received as an isopropanol suspension. To prepare the nanocomposites, the polymer was dissolved in isopropanol and mixed with the Si solution; after sonication, the isopropanol was removed by heating at 80 °C in vacuum. One sample was extracted with hexane for 4 days at RT with gentle stirring and daily solvent replacement, in order to remove the unbound polymer. From thermogravimetric analysis, the silica content increased from 18 to 68 vol %; that is, about 10% of the original polymer was bound. This corresponds to ∼70 attached chains per particle; high grafting densities are known to limit interpenetration by matrix chains.[44]

Dynamic mechanical and shear flow measurements employed an Anton Paar MCR 502 rheometer, using a cone and plate fixture (50 mm diameter with 1° cone angle). Dielectric relaxation spectroscopy was carried out with the sample between cylindrical electrodes (16 mm diameter) with a 0.1 mm separation (Teflon spacer used to maintain constant sample thickness). The permittivity was measured with a Novocontrol Alpha analyzer at frequencies from 10^{-3} to 10^6 Hz. The temperature was controlled using a closed cycle helium cryostat (Cryo Ind.).

RESULTS

Rheology. Figure 1 shows the dynamic viscosity for the neat PPG and four nanocomposites. (The corresponding dynamic moduli are displayed in Figure S1 of the Supporting Information.) At sufficiently high silica loadings, the behavior becomes non-Newtonian. For the highest concentration of silica, there is power law behavior with an exponent ∼0.6. This nonlinearity is seen more clearly in the inset, showing the viscosity as a function of silica volume fraction, ϕ. For spherical particles, the hydrodynamic contribution to the viscosity increase is described by the equation of Guth and Gold[45] as modified for solvation effects[46,47]

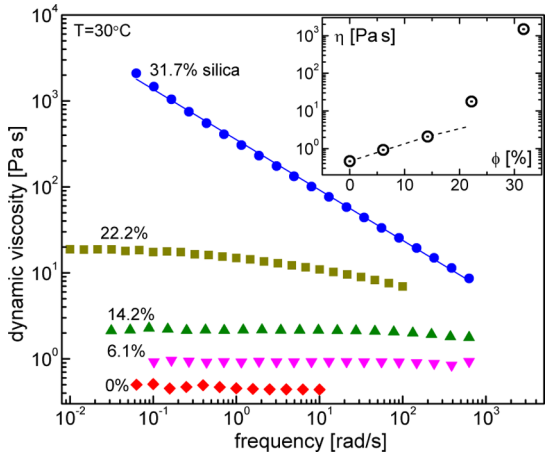

Figure 1. Dynamic viscosity for PPG having the indicated silica concentration. The solid line for the highest silica content is a power-law fit. The inset shows η (0.1 rad/s) vs ϕ. The dashed line is eq 1 fit to the lower filler levels, yielding f = 2.9.

$$\eta(\phi) = \eta_0[1 + 2.5(f\phi) + 14.1(f\phi)^2] \quad (1)$$

where η_0 is the viscosity absent filler, and f accounts the effective "growth" of the particles due to occluded polymer. Fitting eq 1 to the data for $\phi \leq 0.14$, we obtain f = 2.9, which is in the range reported for polymers with conventional reinforcing fillers.[1] The rise in viscosity due to the filler reflects the large hydrodynamic effect from the small particles having enormous interfacial area (the viscosity increase for ϕ = 0.14 is at least 15-fold larger than obtained with conventional silica[48]), augmented by interparticle interactions. The magnitude of the latter can be assessed from nonlinearity in the mechanical response, for example, a strain-dependent dynamic modulus.[49,50] The relatively low molecular weight of the PPG herein, however, permits another approach based on the response to steady shear flow.

As seen in Figure 1, at low levels of silica the PPG exhibits Newtonian behavior. This is the general result for low molecular weight, neat polymers. Materials with time-dependent structure, however, can exhibit stress overshoots and subsequent shear thinning, as the structure is lost upon onset of flow. The most common example of this behavior is flow-induced disentanglement of polymer chains, which causes a transient overshoot upon startup of the shearing.[51−54]

DOI: 10.1021/acs.macromol.6b00354
Macromolecules 2016, 49, 3919−3924

Laboratory characterization of this phenomenon is limited to materials with a low concentration of entanglements; otherwise, there is melt fracture and nonuniform flow.[55,56] Shown in Figure 2 is the transient stress measured for the PPG

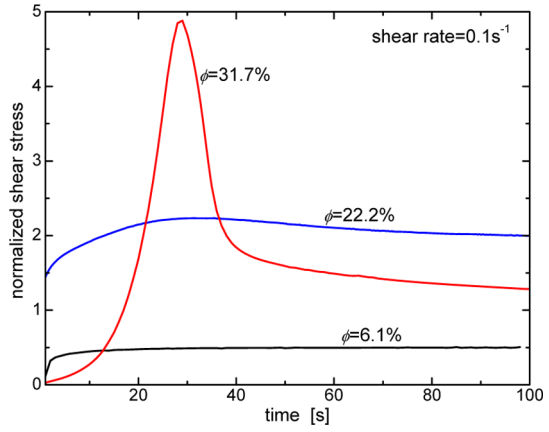

Figure 2. Transient shear stress normalized by the long-time steady-state value (curves displaced vertically for clarity). At higher levels of silica, an overshoot becomes apparent, especially prominent for the largest ϕ. The respective temperatures were chosen to optimize the measurement (T = −50, −20, and 100 °C for lowest to highest concentration); the variation of the overshoot magnitude with temperature is small.

nanocomposites during initiation of steady shear flow. At the highest silica level (ϕ = 0.317) the stress passes through a distinct maximum versus shearing time, followed by a steady-state response. This overshoot peak is also present, albeit weakly, in the PPG with 22.2% silica. These are the two nanocomposites exhibiting shear-thinning behavior in Figure 1. The stress overshoot is absent for samples with less silica.

If the shear flow is stopped and then immediately resumed, there is no maximum in the transient stress. Nevertheless, the disruption of structure underlying the overshoot is a reversible physical process. This is illustrated in Figure 3, showing the transient viscosity, η^+, measured after various rest intervals prior to resumption of the shearing. A time constant, τ, can be obtained for the growth of the overshoot, by describing the

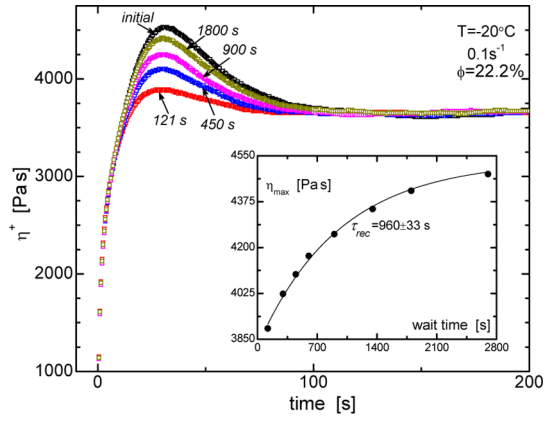

Figure 3. Transient viscosity in the nanocomposite measured after various rest intervals between shearing. The recovery of the overshoot maximum is shown in the inset; the solid line is an exponential fit, yielding the indicated recovery time constant.

peak magnitude, η^+_{max}, measured for various rest times with an exponential function

$$\eta^+_{max}(t) = a\,\exp\left(\frac{-t}{\tau}\right) + \eta^+_{max,\infty} \quad (2)$$

In eq 2, $\eta^+_{max,\infty}$ is the maximum of the transient viscosity after an extended recovery period (exceeding 1 h near ambient temperature for the highest silica concentration studied); $\eta^+_{max,\infty}$ thus equals the value for the initial startup shear flow measurement. The fit of eq 2 to data for ϕ = 0.222 silica is shown in the inset to Figure 3, yielding τ = 960 s at −20 °C. (The temperatures chosen for the experiments reflected the need to have a sufficiently large viscosity and kinetics slow enough for facile measurement.) The steady-state viscosity for this sample at −20 °C was 3.68 kPa s. Estimating a time constant from the Maxwell relation

$$\tau_M = \eta/G_\infty \quad (3)$$

in which G_∞ is the high frequency limiting value of the modulus (∼GPa), we obtain a value ($\tau_M < 10^{-5}$ s) several orders of magnitude smaller than the recovery time. Even given the uncertainty in this τ_M, the implication is that recovery of the overshoot in the transient viscosity cannot be governed by the polymer chain dynamics. To identify the mechanism for the overshoot, in Figure 4 the recovery time constant and the

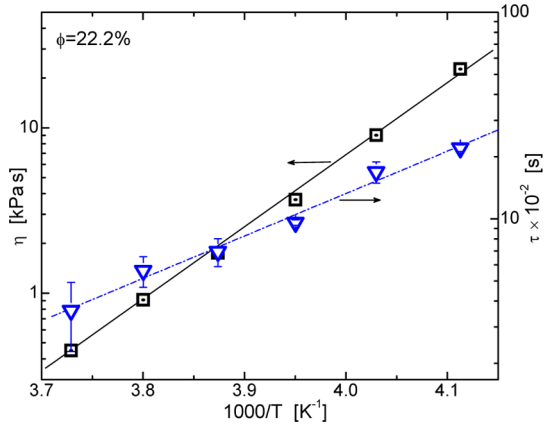

Figure 4. Arrhenius plots for the nanocomposite having the indicated silica volume content: (left axis, squares) viscosity; (right axis, inverted triangles) overshoot recovery time constant. The latter has a 2-fold smaller activation energy.

viscosity are plotted in Arrhenius form. The activation energy for the latter, 83.5 ± 1.6 kJ/mol, is significantly larger than for the overshoot recovery, 39.3 ± 2.2 kJ/mol. This disconnect between the temperature dependences of the two processes is consistent with the idea that that the recovery is not controlled by the chain dynamics. The inference is that particle−particle interactions give rise to a structure that elevates the dynamic viscosity measured at low strain amplitudes (Figure 1); however, the connectivity is fragile, its labile nature yielding an overshoot in the transient viscosity.

Dielectric Relaxation. Since PPG has a dipole moment parallel to the chain, we can further probe the chain dynamics, as well as the local segmental relaxation, using dielectric spectroscopy. In Figure 5 are shown representative dielectric relaxation spectra for the neat PPG and the nanocomposite with ϕ = 0.222; the measurements are at nearly the same temperature. Two peaks are observed, corresponding to the

DOI: 10.1021/acs.macromol.6b00354
Macromolecules 2016, 49, 3919−3924

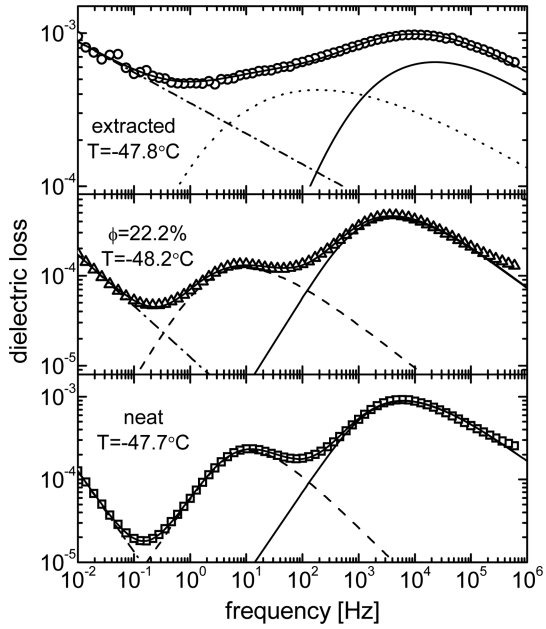

Figure 5. Dielectric spectrum of (bottom to top): neat PPG; nanocomposite; nanocomposite after extraction of unattached polymer. The lines represent fits of the Kohlrausch function to each of the two dispersions, along with a power law at low frequencies due to dc conductivity. The ordinate values are approximate due to sample thickness uncertainties.

local segmental and global chain modes, at higher and lower frequencies, respectively. The Kohlrausch function[57]

$$\varepsilon^*(\nu) = \Delta\varepsilon L\left[-\frac{\mathrm{d}(\exp[-(t/\tau_K)^\beta])}{\mathrm{d}t}\right] \quad (4)$$

is fit to the permittivity spectra, where ν is the frequency, τ_K a mean relaxation time, $\Delta\varepsilon$ the dielectric strength, β the shape parameter, and L indicates the Laplace transform. We simultaneously fit both the real and imaginary part of ε^* for both dispersions, including a term for the dc conductivity, σ_{dc} ($\propto\nu^{-1}$). (Note that the nanocomposites are intrinsically heterogeneous because of the different dielectric properties of the polymer and the particles; however, the effect is weak herein, and correcting for it has a negligible effect on the dielectric spectra.) The normal mode peak is broader for the nanocomposite (β = 0.51) compared to that for neat PPG (β = 0.68), whereas the segmental dispersion (β = 0.50) is unaffected by the silica. The obtained relaxation times are shown in Figure 6. Clearly, there is no observable effect on the average relaxation dynamics due to the presence of the silica particles.

In Figure 7 are shown representative dielectric strength data for the two PPG dispersions. The dielectric strength of the segmental relaxation decreases with increasing silica concentration; however, this decrease exceeds that expected due simply to the reduction in polymer content, a result consistent with the lower than expected density (see below). The dielectric strength of the normal mode is essentially invariant to ϕ. A possible origin of this behavior is an increased end−end distance for the interfacial chains, which would countervail the lower amount of polymer. Such an increase has been observed in molecular dynamics simulations when the polymer interactions with the filler surface are attractive.[34]

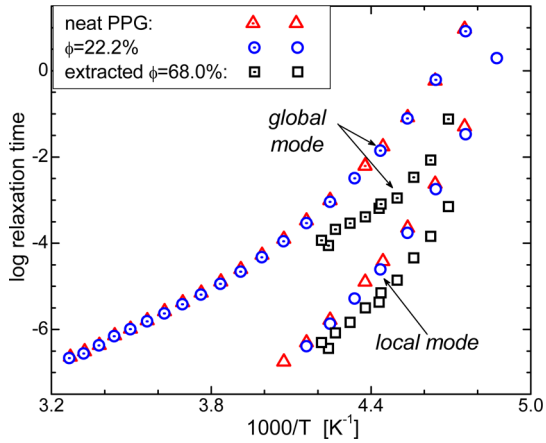

Figure 6. Local segmental (dotted symbols) and dielectric normal mode (open symbols) relaxation times for the neat PPG (triangles), a nanocomposite (circles), and the nanocomposite after extraction of the unbound polymer (squares).

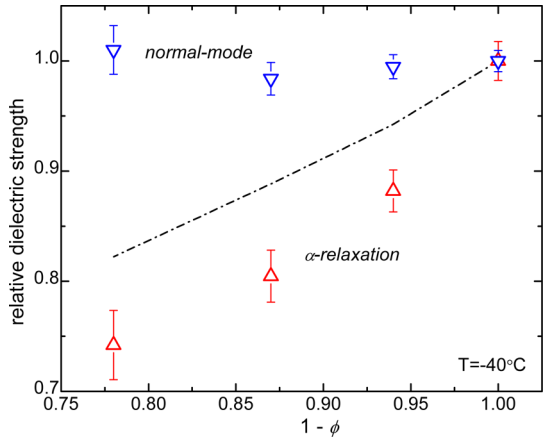

Figure 7. Dielectric strength of the segmental mode (triangles) and normal mode (inverted triangles), normalized by the respective values for neat PPG, as a function of the polymer volume fraction. The dashed line represents the change if the only effect were due to the reduced polymer content of the nanocomposite.

To emphasize the contribution of the interfacial polymer to the dynamic behavior, we extracted the nanocomposite with hexane. This removed all soluble PPG; the remaining polymer (18 wt %) is attached to the silica via the surface hydroxyl groups. The dielectric spectrum of this extracted material, containing only silica and bound PPG, is also shown in Figure 5. Note that the sample lacks mechanical integrity and its bulk density was low; significant compaction could be achieved by application of hydrostatic pressure. However, the shape and peak frequency of the loss spectrum, and by inference the polymer dynamics, were unaffected by transient pressure (see Figure S2). It is evident from the spectra that both the segmental relaxation and the normal mode peaks shift to higher frequency. The speeding up of the dynamics (a result independent of the details of the fitting procedure; see Figure S3) is greater at lower temperatures, with the normal mode relaxation time reduced by as much as a factor of 50. The effect on the segmental mode is smaller but still substantial, about a 5-fold reduction in the relaxation time after extraction. This acceleration of the motions corresponds to temperature increases of about 10 K for the normal mode and 4 K for

DOI: 10.1021/acs.macromol.6b00354
Macromolecules 2016, 49, 3919−3924

the segmental mode. Notwithstanding the greater mobilities, both the local and global relaxation dispersions are much broader for the extracted sample, β = 0.29 and 0.24, respectively.

DISCUSSION AND SUMMARY

Nanoparticles can affect both the local segmental and global dynamics of polymers. Herein silica particles were found to exert a very large effect on the viscosity of PPG and give rise to a prominent overshoot in the transient viscosity during startup of steady shear flow. The retarded recovery of the startup transient indicates it involves interparticle interactions that are largely decoupled from the local viscosity. Notwithstanding these effects of the silica on the rheology of the PPG, the dielectric normal mode measured for the neat PPG and the nanocomposite were equivalent. However, when the unbound polymer was removed by solvent extraction, the global dynamics of the residual PPG, which is adhered to the particles, was found to be more than an order of magnitude faster than for the bulk polymer. A similar result was found for the segmental relaxation, although there was less speeding up of the more local process. To the extent that the local friction factor for the segmental dynamics can be identified with the friction factor governing the global dynamics, as assumed in classical models for the chain dynamics,[58] changes in the two processes should be comparable. However, truncation of the normal modes may underlie the larger effect of the particles on the global motions. If the etheric oxygens in the chain are connected to the silica hydroxyl groups via hydrogen bonds, the normal mode would involve smaller sections of the polymer chain and thus be faster. This would also account for the broader distribution of relaxation times seen for the normal mode. However, if this truncation is the cause of the greater shift of the normal mode peak compared to the segmental relaxation, the difference is artifactual rather than an actual greater enhancement of the global mobility.

Since the segmental dynamics of the bound chains are also faster than for the neat polymer, a second mechanism is also operative. The usual consequence of specific interactions with filler particles, to constrain and retard motions, must be absent herein, or at least overwhelmed by other effects. We can assess the density in the vicinity of the particles by comparing the mass density of the nanocomposite to the prediction assuming additivity of the component volumes. From the densities of the components, ρ = 1.004 and 2.2 g/mL respectively for PPG and silica, we calculate 1.218 g/mL for ϕ = 0.317. We measured, however, 1.12 $\pm$ 0.02 g/mL for this sample; that is, the interface has a significantly lower density than the bulk. This result leads to the conclusion that notwithstanding their being tethered to particles, the interfacial chains experience reduced crowding, presumably the result of poor packing. This would account for faster segmental and chain dynamics.

ASSOCIATED CONTENT

Supporting Information

The Supporting Information is available free of charge on the ACS Publications website at DOI: 10.1021/acs.macromol.6b00354.

Figures S1−S3 (PDF)

AUTHOR INFORMATION

Corresponding Author

*E-mail roland@nrl.navy.mil (C.M.R.).

Notes

The authors declare no competing financial interest.

ACKNOWLEDGMENTS

This work was supported by the Office of Naval Research.

REFERENCES

(1) Armstrong, G. An Introduction to Polymer Nanocomposites. *Eur. J. Phys.* **2015**, *36*, 063001.
(2) Chrissopoulou, K.; Anastasiadis, S. H. Effects of Nanoscopic-Confinement on Polymer Dynamics. *Soft Matter* **2015**, *11*, 3746−3766.
(3) Paul, D. R.; Robeson, L. M. Polymer Nanotechnology: Nanocomposites. *Polymer* **2008**, *49*, 3187−3204.
(4) Hussain, F.; Hojjati, M.; Okamoto, M.; Gorga, R. E. Polymer-Matrix Nanocomposites, Processing, Manufacturing, and Application: An Overview. *J. Compos. Mater.* **2006**, *40*, 1511−1575.
(5) Tjong, S. C. Structural and Mechanical Properties of Polymer Nanocomposites. *Mater. Sci. Eng., R* **2006**, *53*, 73−197.
(6) Hanemann, T.; Szabo, D. V. Polymer-Nanoparticle Composites: From Synthesis to Modern Applications. *Materials* **2010**, *3*, 3468−3517.
(7) Kropka, J. M.; Pryamitsyn, V.; Ganesan, V. Relation between Glass Transition Temperatures in Polymer Nanocomposites and Polymer Thin Films. *Phys. Rev. Lett.* **2008**, *101*, 075702.
(8) Bansal, A.; Yang, H.; Li, C.; Cho, K.; Benicewicz, B. C.; Kumar, S. K.; Schadler, L. S. Quantitative Equivalence Between Polymer Nanocomposites And Thin Polymer Films. *Nat. Mater.* **2005**, *4*, 693−698.
(9) Rittigstein, P.; Priestley, R. D.; Broadbelt, L. J.; Torkelson, J. M. Model Polymer Nanocomposites Provide an Understanding of Confinement Effects in Real Nanocomposites. *Nat. Mater.* **2007**, *6*, 278−282.
(10) Pitsa, D.; Daniaks, M. G. Interfaces Features in Polymer Nanocomposites: A Review of Proposed Models. *Nano* **2011**, *6*, 497−508.
(11) Song, Y. H.; Zheng, W. Linear Rheology of Nanofilled Polymers. *J. Rheol.* **2015**, *59*, 155−191.
(12) Krishnamoorti, R.; Banik, I.; Xu, L. Rheology and Processing of Polymer Nanocomposites. *Rev. Chem. Eng.* **2010**, *26*, 3−12.
(13) Frank, B.; Gast, A. P.; Russell, T. P.; Brown, H. R.; Hawker, C. Polymer Mobility in Thin Films. *Macromolecules* **1996**, *29*, 6531−6534.
(14) Kremer, F.; Hartmann, L.; Serghei, A.; Pouret, P.; Leger, L. Molecular Dynamics in Thin Grafted and Spin-Coated Polymer Layers. *Eur. Phys. J. E: Soft Matter Biol. Phys.* **2003**, *12*, 139−142.
(15) Frieberg, B.; Kim, J.; Narayanan, S.; Green, P. F. Surface Dynamics of Miscible Polymer Blend Nanocomposites. *ACS Nano* **2014**, *8*, 607−613.
(16) Rowland, H. D.; King, W. P.; Pethica, J. B.; Cross, G. L. W. Molecular Confinement Accelerates Deformation of Entangled Polymers During Squeeze Flow. *Science* **2008**, *322*, 720.
(17) Si, L.; Massa, M. V.; Dalnoki-Veress, K.; Brown, H. R.; Jones, R. A. L. Chain Entanglement in Thin Freestanding Polymer Films. *Phys. Rev. Lett.* **2005**, *94*, 127801.
(18) Soles, C. L.; Ding, Y. Nanoscale Polymer Processing. *Science* **2008**, *322*, 689−690.
(19) Karatrantos, A.; Clarke, N.; Composto, R. J.; Winey, K. I. Topological Entanglement Length in Polymer Melts and Nanocomposites by a DPD Polymer Model. *Soft Matter* **2013**, *9*, 3877−3884.
(20) O'Connell, P. A.; McKenna, G. B. Rheological Measurements of the Thermoviscoelastic Response of Ultrathin Polymer Films. *Science* **2005**, *307*, 1760.

DOI: 10.1021/acs.macromol.6b00354
Macromolecules 2016, 49, 3919−3924

(21) Saito, T.; Sakaue, T. Cis-Trans Dynamical Asymmetry in Driven Polymer Translocation. *Phys. Rev. E* **2013**, *88*, 042606.
(22) Dubbeldam, J. L. A.; Rostiashvili, V. G.; Vilgis, T. A. Driven Translocation of a Polymer: Role of Pore Friction and Crowding. *J. Chem. Phys.* **2014**, *141*, 124112.
(23) Lam, P. M.; Zhen, Y. Dynamic Scaling Theory of the Forced Translocation of a Semi-Flexible Polymer Through a Nanopore. *J. Stat. Phys.* **2015**, *161*, 197−209.
(24) de Haan, H. W.; Sean, D.; Slater, G. W. Using a Péclet Number for the Translocation of a Polymer Through a Nanopore to Tune Coarse-Grained Simulations ro Experimental Conditions. *Phys. Rev. E* **2015**, *91*, 022601.
(25) Sarabadani, J.; Ikonen, T.; Ala-Nissila, T. Theory of Polymer Translocation Through a Flickering Nanopore under an Alternating Driving Force. *J. Chem. Phys.* **2015**, *143*, 074905.
(26) Robertson, C. G.; Roland, C. M. Glass Transition and Interfacial Segmental Dynamics in Polymer-Particle Composites. *Rubber Chem. Technol.* **2008**, *81*, 506−522.
(27) Liao, K. H.; Aoyama, S.; Abdala, A. A.; Macosko, C. Does Graphene Change T_g of Nanocomposites? *Macromolecules* **2014**, *47*, 8311−8319.
(28) Ganesan, V.; Jayaraman, A. Theory and Simulation Studies of Effective Interactions, Phase Behavior and Morphology in Polymer Nanocomposites. *Soft Matter* **2014**, *10*, 13−38.
(29) Adnan, A.; Sun, C. T.; Mahfuz, H. *Compos. Sci. Technol.* **2007**, *67*, 348−356.
(30) Starr, F. W.; Douglas, J. F. Modifying Fragility and Collective Motion in Polymer Melts with Nanoparticles. *Phys. Rev. Lett.* **2011**, *106*, 115702.
(31) Liu, J.; Wu, Y.; Shen, J.; Gao, Y.; Zhang, L.; Cao, D. Polymer−Nanoparticle Interfacial Behavior Revisited: A Molecular Dynamics Study. *Phys. Chem. Chem. Phys.* **2011**, *13*, 13058−13069.
(32) Brown, D.; Marcadon, V.; Mele, P.; Alberola, N. D. Effect of Filler Particle Size On The Properties Of Model Nanocomposites. *Macromolecules* **2008**, *41*, 1499.
(33) Smith, J. S.; Borodin, O.; Smith, G. D.; Kober, E. M. A Molecular Dynamics Simulation and Quantum Chemistry Study of Poly(dimethylsiloxane)-Silica Nanoparticle Interactions. *J. Polym. Sci., Part B: Polym. Phys.* **2007**, *45*, 1599.
(34) Karatrantos, A.; Clarke, N.; Composto, R. J.; Winey, K. I. Polymer Conformations in Polymer Nanocomposites Containing Spherical Nanoparticles. *Soft Matter* **2015**, *11*, 382−388.
(35) Kalathi, J. T.; Kumar, S. K.; Rubinstein, M.; Grest, G. S. Rouse Mode Analysis of Chain Relaxation in Polymer Nanocomposites. *Soft Matter* **2015**, *11*, 4123−4132.
(36) Holt, A.; Sangoro, J. R.; Wang, Y.; Agapov, A. L.; Sokolov, A. P. Chain and Segmental Dynamics of Poly (2-Vinylpyridine) Nanocomposites. *Macromolecules* **2013**, *46*, 4168−4173.
(37) Moll, J.; Kumar, S. K. Glass Transitions in Highly Attractive Highly Filled Polymer Nanocomposites. *Macromolecules* **2012**, *45*, 1131−1135.
(38) Robertson, C. G.; Lin, C. J.; Bogoslovov, R. B.; Rakaitis, M.; Sadhukhan, P.; Quinn, J. D.; Roland, C. M. Flocculation, Reinforcement, and Glass Transition Effects in Silica-Filled Styrene-Butadiene Rubber. *Rubber Chem. Technol.* **2011**, *84*, 507−519.
(39) Cheng, S.; Mirigian, S.; Carrillo, J.-M. Y.; Bocharova, V.; Sumpter, B. G.; Schweizer, K. S.; Sokolov, A. P. Revealing Spatially Heterogeneous Relaxation in a Model Nanocomposite. arXiv:1509.00688, 2015.
(40) Gong, S.; Chen, Q.; Moll, J. F.; Kumar, S. K.; Colby, R. H. Segmental Dynamics of Polymer Melts with Spherical Nanoparticles. *ACS Macro Lett.* **2014**, *3*, 773−777.
(41) Bogoslovov, R. B.; Roland, C. M.; Ellis, A. R.; Randall, A. M.; Robertson, C. G. *Macromolecules* **2008**, *41*, 1289−1296.
(42) Tadiello, L.; D'Arienzo, M.; Di Credico, B.; Hanel, T.; Matejka, L.; Mauri, M.; Morazzoni, F.; Simonutti, R.; Spirkova, M.; Scotti, R. *Soft Matter* **2015**, *11*, 4022−4033.
(43) Masui, T.; Kishimoto, H.; Kikuchi, T.; Ohira-Kawamura, S.; Inamura, Y.; Koga, T.; Nakajima, K. *J. Phys.: Conf. Ser.* **2014**, *502*, 012507.
(44) Green, P. F. The Structure of Chain End-Grafted Nanoparticle/Homopolymer Nanocomposites. *Soft Matter* **2011**, *7*, 7914−7926.
(45) Guth, E.; Gold, O. On the Hydrodynamical Theory of the Viscosity of Suspensions. *Phys. Rev. E* **1938**, *53*, 322−322.
(46) Medalia, A. I. Effective Degree of Immobilization of Rubber Occluded within Carbon Black Aggregates. *Rubber Chem. Technol.* **1972**, *45*, 1171−1194.
(47) Fukahori, Y.; Hon, A. A.; Jha, V.; Busfield, J. J. C. Modified Guth-Gold Equation for Carbon Black-Filled Rubbers. *Rubber Chem. Technol.* **2013**, *86*, 218−232.
(48) Roy, D.; Casalini, R.; Roland, C. M. Local and Global Dynamics in Polypropylene Glycol/Silica Composites. *Soft Matter* **2015**, *11*, 9379−9384.
(49) Payne, A. R. The Dynamic Properties of Carbon Black-Loaded Natural Rubber Vulcanizates. Part I. *J. Appl. Polym. Sci.* **1962**, *6*, 57−63.
(50) Roland, C. M.; Lee, G. F. Interaggregate Interaction in Filled Rubber. *Rubber Chem. Technol.* **1990**, *63*, 554−566.
(51) Stratton, R. A.; Butcher, A. F. Stress Relaxation upon Cessation of Steady Flow and the Overshoot Effect of Polymer Solutions. *J. Polym. Sci. Polym. Phys. Ed.* **1973**, *11*, 1747−1758.
(52) Menezes, E. V.; Graessley, W. W. Nonlinear Rheological Behavior of Polymer Systems for Several Shear-Flow Histories. *J. Polym. Sci., Polym. Phys. Ed.* **1982**, *20*, 1817−1833.
(53) Robertson, C. G.; Warren, S.; Plazek, D. J.; Roland, C. M. Reentanglement Kinetics in Sheared Polybutadiene Solutions. *Macromolecules* **2004**, *37*, 10018−10022.
(54) Roy, D.; Roland, C. M. Reentanglement Kinetics in Polyisobutylene. *Macromolecules* **2013**, *46*, 9403−9408.
(55) Sui, C.; McKenna, G. B. Instability of Entangled Polymers in Cone and Plate Rheometry. *Rheol. Acta* **2007**, *46*, 877−888.
(56) Inn, Y. W.; Wissbrun, K. F.; Denn, M. M. Effect of Edge Fracture on Constant Torque Rheometry of Entangled Polymer Solutions. *Macromolecules* **2005**, *38*, 9385−9388.
(57) Kremer, F., Schonhals, A., Eds.; *Broadband Dielectric Spectroscopy*; Springer: Berlin, 2003.
(58) Roland, C. M. *Viscoelastic Behavior of Rubbery Materials*; Oxford Univ. Press: Oxford, 2011.

DOI: 10.1021/acs.macromol.6b00354
Macromolecules 2016, 49, 3919−3924

Macromolecules

Addition/Correction

pubs.acs.org/Macromolecules

Correction to Local and Global Dynamics in Polypropylene Glycol/Silica Composites

R. Casalini and C. M. Roland*

Macromolecules **2016**, *49* (10), 3919−3924. DOI: 10.1021/acs.macromol.6b00354

Equation 2 in our recent publication[1] was in error; the corrected version is

$$\eta^{+}_{\max}(t) = a \exp\left(\frac{t}{\tau}\right) + \eta^{+}_{\max,\infty} \tag{2}$$

We thank Prof. G. G. Lin (Tamkang Univ.) for pointing out the error.

REFERENCES

(1) Casalini, R.; Roland, C. M. Local and Global Dynamics in Polypropylene Glycol/Silica Composites. *Macromolecules* **2016**, *49*, 3919−3924.

DOI: 10.1021/acs.macromol.7b00053
Macromolecules XXXX, XXX, XXX−XXX

SUPPORTING INFORMATION

Local and global dynamics in polypropylene glycol / silica composites

R. Casalini and C.M. Roland
Naval Research Laboratory, Chemistry Division, Washington DC 20375-5342

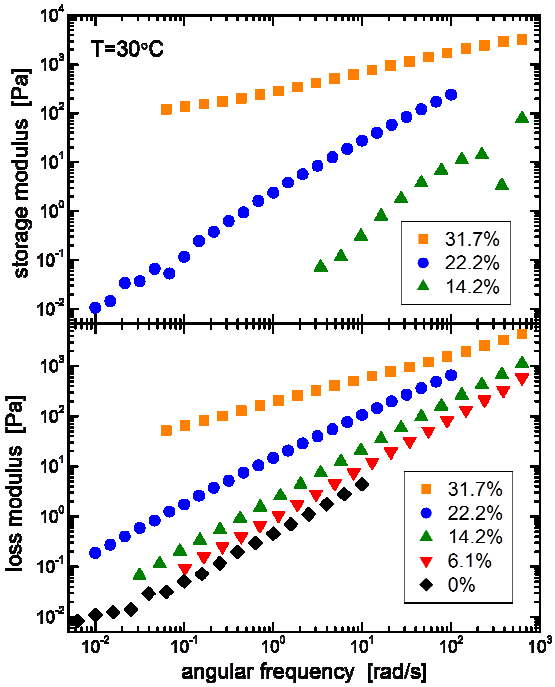

Figure S1. Dynamic moduli of PPG with the indicated volume content of silica.

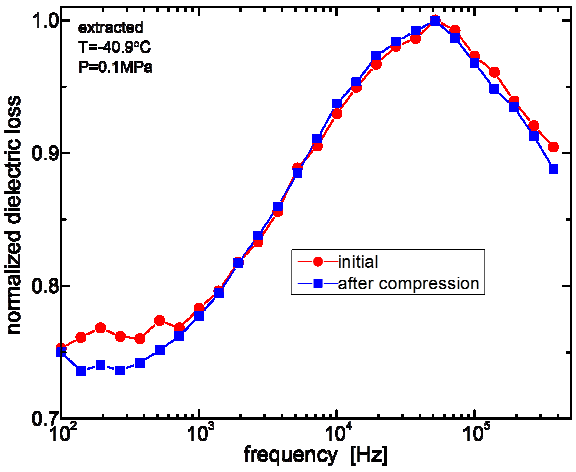

Figure S2. Dielectric loss of the extracted nanocomposite as prepared (circles) and after application and removal of 16 MPa hydrostatic pressure (squares); both spectra have been normalized by the peak maximum. Transient pressure compacts the sample, increasing the bulk density and apparent dielectric strength by a factor of 2.3. However, the equivalence of the spectral frequencies and shapes shows the absence of any change in dynamics of the interfacial polymer.

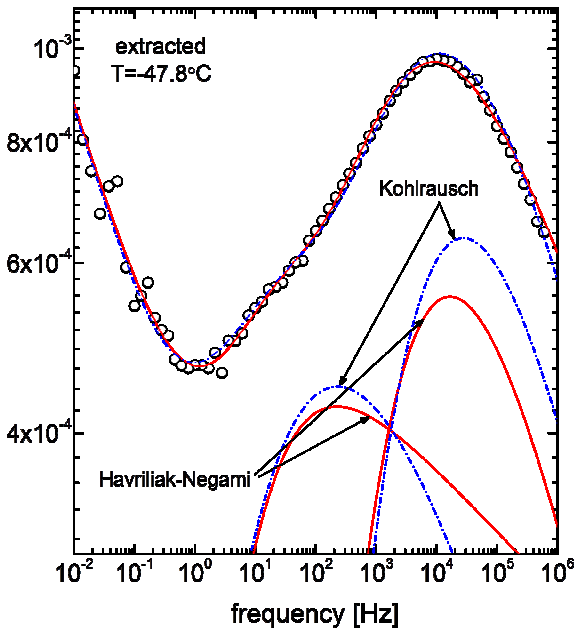

Figure S3. Comparison of fitting the lower frequency normal mode peak with the transform of the Kohlrausch function (dashed lines) or the Havriliak-Negami equation (solid line). The fits are almost equivalent: The most probable α-relaxation time changes by 1%, and the normal mode relaxation time changes by 60%, both much smaller than the changes in these relaxation times due to extraction of unbound polymer (which is a factor of about 170 at this temperature).